

Chapter 5

Other Interesting Topics

5.1 Introduction

This chapter comprises a series of topics which are of general interest and extend the range of applications of boundary elements but are not as essential as those described in previous chapters to understand the method.

One of the most interesting possibilities of boundary elements is that it is easy to combine the technique with other numerical methods. The range of combinations varies from those needed in analysis where boundary layers are interfaced to boundary element regions, to simple coupling in static analysis. Sometimes for instance, matrices for potential fluids are formed using boundary elements and combined with finite element models for shells which represent a container, an aerospace structure, an offshore platform, etc. The coupling is particularly simple as boundary elements accept discontinuity of variables and full compatibility is not required to obtain accurate answers. Ways of combining finite and boundary elements are particularly attractive in view of the widespread use of both methods. Although many papers have been published on the topic, section 5.2 only discusses comparatively simple ways of carrying out this combination. The first technique is a purely intuitive approach which is not justified mathematically. It consists of using the finite element results from a global solution as boundary conditions when focusing on a particular region of the system. The finite element boundary variables used are potentials or displacements as they are given with a higher order of accuracy than fluxes or tractions.

The first of the other two approaches consists of treating the boundary element region as a finite element and appropriately transforming the matrices. The second approach consists of treating the finite element region as a boundary element and manipulating the FE matrices in such a way that they can be implemented in the boundary element system. Both approaches give similar results and using one or the other will depend on which part of the problem (i.e. finite or boundary element parts) is predominant.

Section 5.3 discusses special types of boundary element, which are produced by asymptotic considerations when the boundary is far from the part under perturbation. Under certain hypotheses these elements are equivalent to the radiation type conditions presented by different authors. The section gives a methodology of how these conditions can be obtained from basic boundary integral considerations.

One of the first applications of boundary elements was the study of elastic fracture mechanics problems for which singularities arise at the tip of the crack.

These problems have been solved by different authors using a variety of boundary integral formulations but more recently they have been studied using a simple transformation which produces a singularity at the tip of the crack. This is achieved by using the so-called quarter point elements which were first developed for finite elements. They give a very elegant formulation in the case of boundary elements, which directly produce the stress intensity coefficients in a way that can not be done using finite elements.

The last section in this chapter explains how the technique can be expanded to study steady state elastodynamics problems. Although this is similar to what has been shown in Chapter 2 for the Helmholtz equation (section 2.14) it was decided to include this amongst the special topics as the frequency dependent formulation in elasticity is rather complex.

In spite of that, the implementation of the resulting relationships in existing elastostatics codes (including those presented in Chapter 4 of this book) can be attempted by the reader as explained in section 5.5.

5.2 Combination of Boundary and Finite Elements

There are sometimes advantages in combining finite and boundary element solutions. In many unbounded field problems for instance, boundary elements may provide the appropriate conditions to represent the infinite domain while finite elements can solve complex material properties in the near domain. Boundary elements are also of interest in regions of high stresses or potentials, but finite elements may be adequate for other parts of the boundary and may be simpler to use in cases such as layered continuum, anisotropic and non-linear materials. Hence it is important for the analyst to be able to represent a body using finite or boundary element techniques, depending on the particular geometries or boundary conditions.

There are many papers written on the combination of the two techniques, but from the viewpoint of simplicity of application as it relates to the codes already described here, we will consider only three methods, i.e.

- (i) *Method (i)* Using the finite element solution to define the boundary conditions for a localized boundary element region.
- (ii) *Method (ii)* Treating a boundary element region as a finite element and combining with finite elements.
- (iii) *Method (iii)* The converse of method (ii), i.e. treating a finite element region as an equivalent boundary element and combining with the other boundary element region.

Method (i) This approach is a purely empirical technique and consists of having solved a problem using finite elements to 'zoom' in a particular region using as boundary conditions the finite element results for displacements or potentials.

The approach can not easily be justified from a mathematical standpoint but it is used in several codes and seems to produce reasonable results. One can apply

this technique in the case of studying a region with a crack as shown in figure 5.1. First a global finite element solution is found using the mesh described in figure 5.1(a) and then the boundary element method is used to study the crack region in more detail as shown in figure 5.1(b) using as boundary conditions the displacements obtained in the finite element code. The reason why the approach works is due to the fact that the finite element results for displacements (or potentials) are usually accurate. The method would not give good results if the finite element stresses (or fluxes) were used instead.

Method (ii) The second approach consists in treating the boundary element region as a finite element. Consider the two regions as shown in figure 5.2 where region Ω^1 is expressed in terms of boundary solutions and Ω^2 discretized into finite elements.

The boundary element matrices for Ω^1 can be written as

$$\mathbf{HU} = \mathbf{GP} \quad (5.1)$$

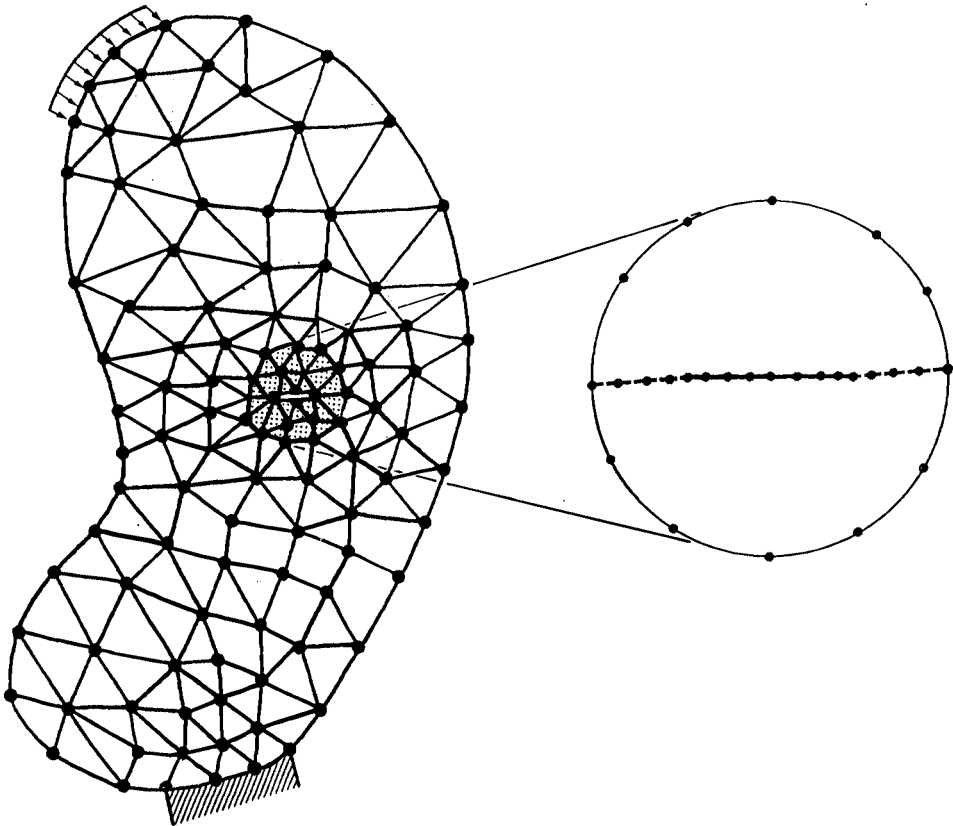


Figure 5.1. Method (i) combining global finite element solution with a localized boundary element region

while for region Ω^2 the finite element matrices are

$$\mathbf{K}\mathbf{U} = \mathbf{F} \quad (5.2)$$

where \mathbf{K} is the stiffness matrix of the problem and \mathbf{F} the *equivalent* nodal forces. Note that \mathbf{U} represents the displacements (or potentials) and \mathbf{P} are the surface tractions (or fluxes).

In order to combine (5.1) and (5.2) one can reduce the first to a finite element form by inverting \mathbf{G} , i.e.

$$\mathbf{G}^{-1}\mathbf{H}\mathbf{U} = \mathbf{P} \quad (5.3)$$

Next one can convert the values of tractions at the nodes (as given by \mathbf{P}) into an equivalent nodal force matrix of the type used in finite elements. This is done by weighting the boundary tractions by the interpolation function used for the displacements and produces a matrix \mathbf{M} such that

$$\mathbf{F} = \mathbf{M}\mathbf{P} \quad (5.4)$$

This operation is standard in finite elements although it is unusual to write the distribution matrix \mathbf{M} in an explicit form.

Equation (5.3) can now be written as

$$\mathbf{M}(\mathbf{G}^{-1}\mathbf{H})\mathbf{U} = \mathbf{M}\mathbf{P} = \mathbf{F}' \quad (5.5)$$

where the right hand side vector has the same form as in finite elements.

One can now write formula (5.5) as

$$\mathbf{K}'\mathbf{U} = \mathbf{F}' \quad (5.6)$$

where $\mathbf{K}' = \mathbf{M}\mathbf{G}^{-1}\mathbf{H}$.

\mathbf{K}' is a stiffness matrix obtained from the boundary element formulation. It is generally asymmetric due to the approximations involved in the discretization process and the choice of the assumed solution. Although this matrix is sometimes symmetrized simply taking an average of the off-diagonal terms (i.e. assuming it can be written as $\frac{1}{2}(\mathbf{K}' + \mathbf{K}'^T)$) this is not recommended as it produces inaccurate results in many practical applications. Obtaining symmetric boundary element stiffness matrices may involve double integration of the type used in Galerkin's BE formulation which are beyond the scope of this book.

The equivalent finite element type matrices of equation (5.6) can now be assembled with the matrices corresponding to region Ω^2 in figure 5.2 to form the global stiffness matrix.

Method (iii) This approach was proposed by Brebbia and Georgiou in 1979 [1] and consists in treating the finite element region as an equivalent boundary element.

Consider the two regions described in figure 5.2. For region 1 one can write the governing equations in a manner similar to that previously shown for multiregion problems, i.e.

$$[\mathbf{H}^1 \quad \mathbf{H}_I^1] \begin{Bmatrix} \mathbf{U}^1 \\ \mathbf{U}_I^1 \end{Bmatrix} = [\mathbf{G}^1 \quad \mathbf{G}_I^1] \begin{Bmatrix} \mathbf{P}^1 \\ \mathbf{P}_I^1 \end{Bmatrix} \quad (5.7)$$

where the subscript I defines the interface.

The matrices for the finite element region 2 can be written in a similar manner using the concept of distribution matrix defined in formula (5.4), i.e.

$$[\mathbf{K}^2 \quad \mathbf{K}_I^2] \begin{Bmatrix} \mathbf{U}^2 \\ \mathbf{U}_I^2 \end{Bmatrix} = [\mathbf{M}^2 \quad \mathbf{M}_I^2] \begin{Bmatrix} \mathbf{P}^2 \\ \mathbf{P}_I^2 \end{Bmatrix} \quad (5.8)$$

By writing $\mathbf{P}_I = \mathbf{P}_I^1 = -\mathbf{P}_I^2$ and $\mathbf{U}_I = \mathbf{U}_I^1 = \mathbf{U}_I^2$ one automatically satisfies the equilibrium and compatibility conditions on the interface and equation (5.7) and (5.8) can be rearranged and written together as follows.

$$\begin{bmatrix} \mathbf{H}^1 & \mathbf{H}_I^1 & -\mathbf{G}_I^1 & \mathbf{0} \\ \mathbf{0} & \mathbf{K}_I^2 & \mathbf{M}_I^2 & \mathbf{K}^2 \end{bmatrix} \begin{Bmatrix} \mathbf{U}^1 \\ \mathbf{U}_I \\ \mathbf{P}_I \\ \mathbf{U}^2 \end{Bmatrix} = \begin{bmatrix} \mathbf{G}^1 & \mathbf{0} \\ \mathbf{0} & \mathbf{M}^2 \end{bmatrix} \begin{Bmatrix} \mathbf{P}^1 \\ \mathbf{P}^2 \end{Bmatrix} \quad (5.9)$$

These equations will of course need to be rearranged in accordance with the boundary conditions. Notice that this approach does not require any matrix inversion.

Method (ii) – without forced symmetrization – and method (iii) are equivalent and give the same numerical results. Using one or the other depends mainly upon the problem in the sense of which part is more dominant, the finite elements or the boundary elements, in which case one can use method (ii) or (iii) respectively.

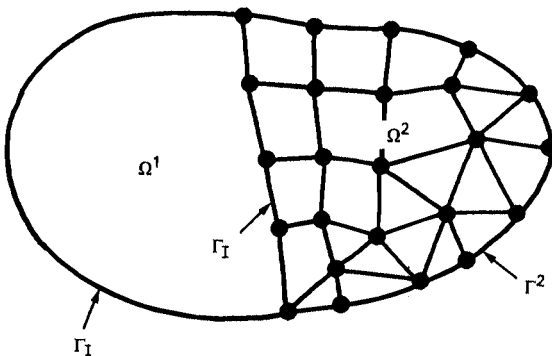


Figure 5.2 Boundary divided into a finite elements and a boundary element region

Method (ii) is essentially a stiffness method and can easily be incorporated in existing finite element packages, although it does require the inversion of the non-banded \mathbf{G} matrix. In contrast, method (iii) does not require this inversion and both displacements and tractions remain unknown along the interface.

5.3 Approximate Boundary Elements

Combination of boundary elements with finite elements is particularly useful when dealing with domains tending to infinity. In these cases the near region is discretized into finite elements and the outside domain is simulated with the boundary elements on the interface of the two regions. This avoids having to discretize a larger region and at a certain distance putting some boundary conditions which try to represent the domain going to infinity. The main drawback of this approach however, is that the boundary element matrices are fully populated representing coupling of all the nodes on the boundary. In practice this coupling can be avoided by assuming that far from the region being perturbed the solution behaves in a smooth manner. This produces an approximate boundary element formulation that in many cases is equivalent to the use of radiation or similar boundary conditions. It is important to point out that these approximate boundary elements are not related to the so-called infinite elements which are based on domain rather than boundary integration.

Consider the example shown in figure 5.3 where the internal region is assumed to be subdivided into finite elements and the external region extending to infinity is modelled using boundary elements. Let us consider that the problem is governed by the Laplace's equation and hence the fundamental solution for two dimensions is

$$u^* = \frac{1}{2\pi} \ln\left(\frac{1}{r}\right) \quad (5.10)$$

For any point in the internal domain (including those near but not on the Γ_I interface) one can write,

$$\int_{\Gamma_I} u^* q \, d\Gamma = \int_{\Gamma_I} u q^* \, d\Gamma \quad (5.11)$$

Substituting the fundamental solution (5.10) into (5.11) leads to

$$\int_{\Gamma_I} \ln\left(\frac{1}{r}\right) q \, d\Gamma = \int_{\Gamma_I} u \frac{\partial}{\partial n} \left(\ln\left(\frac{1}{r}\right) \right) d\Gamma \quad (5.12)$$

Notice that the reference point is considered to be outside the external region and hence $c_i = 0$. The integration still needs to be carried out over all the Γ_I interfaces and all u and q values are interrelated. One can simplify the formulation however, if Γ_I is considered to be a circle of sufficiently large radius R which is assumed to be constant, hence $d\Gamma = R \, d\theta$, where θ is the angular coordinate. Notice also that

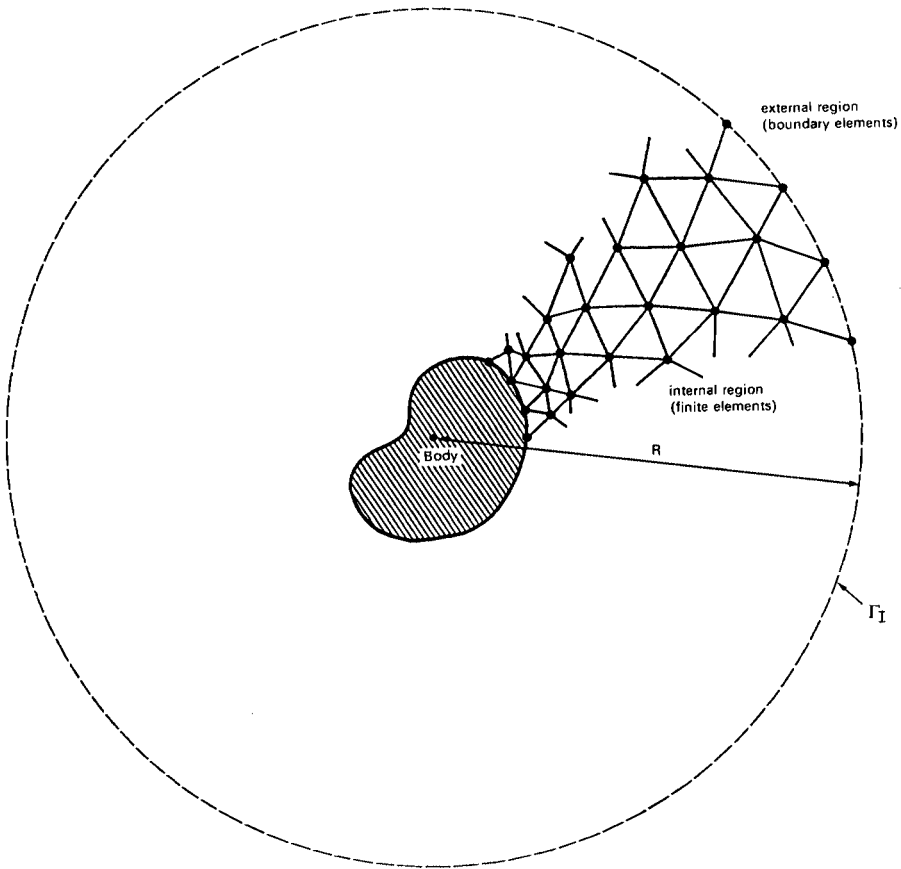


Figure 5.3 Finite and boundary element regions

$n \cong r$ if the reference point is far from the boundary Γ_I and hence equation (5.12) can be written as

$$\int_0^{2\pi} \left(\ln \frac{1}{r} \frac{\partial u}{\partial n} + u \frac{1}{r} \right) d\theta = 0 \tag{5.13}$$

$q = \partial u / \partial r$.

This is a special form of the Sommerfeld condition which can also be written as,

$$\frac{1}{r} u = (\ln r) \frac{\partial u}{\partial r} \quad \text{on } \Gamma_I \tag{5.14}$$

Applying similar considerations for three dimensional potential problems one finds another form of this condition, i.e.

$$\frac{\partial u}{\partial r} + \frac{1}{r} u = 0 \quad \text{on } \Gamma_I \tag{5.15}$$

The above radiation condition can then be applied as a boundary condition for the finite element model describing the internal region.

The interesting aspect of this procedure is that it can be generalized to find approximate radiation conditions in cases where the fundamental solution is complex. Brebbia and Walker [2] have shown how given the Helmholtz equation

$$\nabla^2 u + \kappa^2 u = 0 \quad (5.16)$$

where κ is the wave number and u the potential, the corresponding approximate boundary elements (or radiation condition) on Γ_I are

$$\frac{\partial u}{\partial n} + i\kappa u = 0 \quad \text{on } \Gamma_I \quad (5.17)$$

The demonstration follows the same steps as the one above.

Applications for wave diffraction problems demonstrate that the results obtained using this approach are accurate. Other applications include harbour resonance problems also governed by the Helmholtz equation [2] and soil dynamics problems.

5.4 Singular Elements for Fracture Mechanics

Several approaches have been proposed in finite and boundary elements to model the singular behaviour of stresses at a crack tip which occurs in elastic materials. It is well known that the stresses near a traction free crack in an in-plane loaded plate can be written as, [3]

$$\begin{aligned} \sigma_{11} &= \frac{K_I}{\sqrt{(2\pi r)}} \cos \frac{\theta}{2} \left(1 - \sin \frac{\theta}{2} \sin \frac{3}{2} \theta \right) - \frac{K_{II}}{\sqrt{(2\pi r)}} \sin \frac{\theta}{2} \left(2 + \cos \frac{\theta}{2} \cos \frac{3}{2} \theta \right) \\ \sigma_{22} &= \frac{K_I}{\sqrt{(2\pi r)}} \cos \frac{\theta}{2} \left(1 + \sin \frac{\theta}{2} \sin \frac{3}{2} \theta \right) + \frac{K_{II}}{\sqrt{(2\pi r)}} \cos \frac{\theta}{2} \sin \frac{\theta}{2} \cos \frac{3}{2} \theta \\ \sigma_{12} &= \frac{K_I}{\sqrt{(2\pi r)}} \sin \frac{\theta}{2} \cos \frac{\theta}{2} \cos \frac{3}{2} \theta + \frac{K_{II}}{\sqrt{(2\pi r)}} \cos \frac{\theta}{2} \left(1 - \sin \frac{\theta}{2} \sin \frac{3}{2} \theta \right) \end{aligned} \quad (5.18)$$

where r and θ are defined in figure 5.4, K_I and K_{II} are the stress intensity factors corresponding to the opening and sliding mode, respectively, and the size of r is much smaller than the crack length. The displacements near the crack tip are,

$$\begin{aligned} u_1 &= \frac{K_I}{\mu} \sqrt{\left(\frac{r}{2\pi}\right)} \cos \frac{\theta}{2} \left(1 - 2\nu + \sin^2 \frac{\theta}{2} \right) + \frac{K_{II}}{\mu} \sqrt{\left(\frac{r}{2\pi}\right)} \sin \frac{\theta}{2} \left(2 - 2\nu + \cos^2 \frac{\theta}{2} \right) \\ u_2 &= \frac{K_I}{\mu} \sqrt{\left(\frac{r}{2\pi}\right)} \sin \frac{\theta}{2} \left(2 - 2\nu - \cos^2 \frac{\theta}{2} \right) + \frac{K_{II}}{\mu} \sqrt{\left(\frac{r}{2\pi}\right)} \cos \frac{\theta}{2} \left(-1 + 2\nu + \sin^2 \frac{\theta}{2} \right) \end{aligned} \quad (5.19)$$

where μ is the shear modulus and ν the Poisson ratio as in plane strain problems. Formulae (5.18) and (5.19) describe the stress and displacement distribution near the crack tip and have been obtained analytically. Values of K_I and K_{II} are difficult to obtain for general cases and it is then important to be able to model the behaviour of cracks in boundary element codes.

Snyder and Cruse [4], Stern *et al.* [5] and Cruse [6] presented several procedures to compute stress intensity factors using boundary elements, in particular a singular quarter-point boundary element was proposed by Blandford *et al.* [7] and by Martinez and Dominguez [8]. While some of the approaches proposed are complex to implement, the quarter point element is easy to use in boundary elements, gives accurate results and is no way sensitive to the discretization used. As with other boundary element techniques, the domain needs to be divided into subdomains by means of interfaces (figure 5.5) starting at the crack tip in order to avoid having two similar sets of equations which will produce a singular matrix. This subdivision avoids the numerical problems derived from having two displacement variables for the same geometrical point along the crack. All boundaries are discretized into elements and elements are also defined along the two faces of the crack and the interfaces between different regions. Boundary conditions are applied at external boundaries including zero traction conditions along the crack and the usual equilibrium and compatibility requirements are satisfied at the interfaces.

The quarter point element is based on the quadratic expansion. In this case any displacement, traction or coordinate such as x_1 and x_2 can be represented as

$$\mathbf{f} = \phi \mathbf{f}^j \quad (5.20)$$

where f represents geometrical displacements or traction variables as seen in equations (4.51) to (4.54) and ϕ are the quadratic shape function matrices. Any of these components can be written as,

$$f_i = \phi_1 f_i^1 + \phi_2 f_i^2 + \phi_3 f_i^3 \quad (5.21)$$

For the particular case that the quadratic element has a straight-line geometry and the mid-node is placed at a quarter of the length (figure 5.6) a simple relationship can be found between the coordinate ξ and the variable \bar{r} along the element. In this case equation (5.21) gives

$$f_i = a_i^1 + a_i^2 \sqrt{\frac{\bar{r}}{l}} + a_i^3 \frac{\bar{r}}{l} \quad (5.22)$$

where

$$\begin{aligned} a_i^1 &= f_i^1 \\ a_i^2 &= -f_i^3 + 4f_i^2 - 3f_i^1 \\ a_i^3 &= 2f_i^3 - 4f_i^2 + 2f_i^1 \end{aligned} \quad (5.23)$$

Equation (5.22) ensures that for this position of the mid-point, the $\sqrt{\bar{r}}$ behaviour

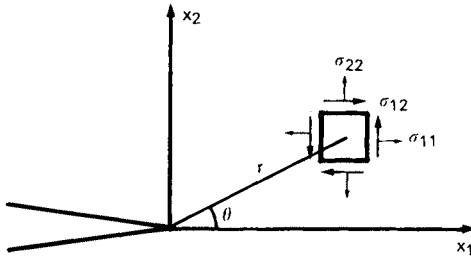


Figure 5.4 Coordinates near the tip

of the displacement near the crack tip as given by equation (5.19) is reproduced by the boundary element. This type of element is usually known as the 'quarter-point element'.

Since in the BEM displacements and tractions are represented independently, a correct representation of the displacements is compatible with an incorrect representation of the tractions. However, the singularity may be included in the representation of the tractions by using modified shape functions. Assume, for instance, that the crack tip is at node 1 (figure 5.6). One may write,

$$p_i = \phi_1 \bar{p}_i^1 \sqrt{\frac{l}{r}} + \phi_2 \bar{p}_i^2 \sqrt{\frac{l}{r}} + \phi_3 \bar{p}_i^3 \sqrt{\frac{l}{r}} \quad (5.24)$$

or

$$p_i = \bar{\phi}_1 \bar{p}_i^1 + \bar{\phi}_2 \bar{p}_i^2 + \bar{\phi}_3 \bar{p}_i^3 \quad (5.25)$$

where $\bar{\phi}_1$, $\bar{\phi}_2$ and $\bar{\phi}_3$ are the modified shape functions which include the $r^{-1/2}$ singularity. Now \bar{p}_i^j stands for the value of p_i at node j divided by the value of $\bar{\phi}_i$ at that node; i.e.,

$$\bar{p}_i^3 = p_i^3$$

$$\bar{p}_i^2 = p_i^2/2$$

$$\bar{p}_i^1 = \lim_{r \rightarrow 0} p_i^1 \sqrt{\frac{r}{l}}$$

Equation (5.24) for p_i can now be written as

$$p_i = \bar{a}_i^1 \sqrt{\frac{l}{r}} + \bar{a}_i^2 + \bar{a}_i^3 \sqrt{\frac{r}{l}} \quad (5.26)$$

where $\bar{a}_i^1 = \bar{p}_i^1$; $\bar{a}_i^2 = -\bar{p}_i^3 + 4\bar{p}_i^2 - 3\bar{p}_i^1$ and $\bar{a}_i^3 = 2\bar{p}_i^3 - 4\bar{p}_i^2 + 2\bar{p}_i^1$.

Using the quarter-point element with the shape functions of equation (5.25) for the tractions, both displacements and tractions will be correctly represented. The element including this kind of representation is known as the traction singular quarter-point element.

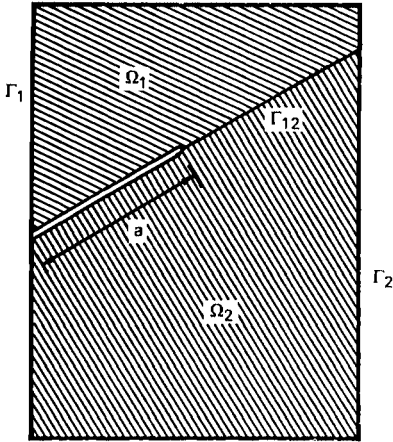


Figure 5.5 Edge cracked plate

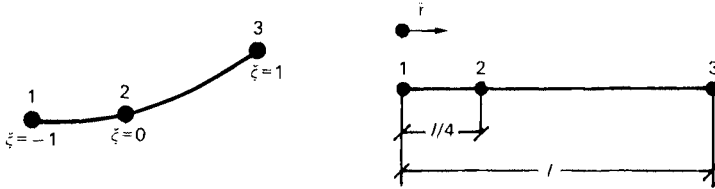


Figure 5.6 Quadratic and quadratic quarter point elements

The first and second mode stress intensity factors can be defined by the following limits (figure 5.4).

$$\begin{aligned}
 K_I &= \lim_{x_1 \rightarrow 0} \{ \sqrt{2\pi x_1} \sigma_{22} \} \\
 K_{II} &= \lim_{x_1 \rightarrow 0} \{ \sqrt{2\pi x_1} \sigma_{12} \}
 \end{aligned}
 \tag{5.27}$$

If the boundary discretization is done in such a way that the first interface element from the crack tip has $\theta = 0^\circ$ and this element is a singular quarter-point boundary element, then for this element, $\bar{r} \equiv x_1$, $p_1 \equiv \sigma_{12}$, $p_2 \equiv \sigma_{22}$ and the nodal values for the tractions at the tip node K are:

$$\begin{aligned}
 \bar{p}_1^k &= \lim_{\bar{r} \rightarrow 0} \{ p_1^k \sqrt{\bar{r}/l} \} = \lim_{x_1 \rightarrow 0} \{ \sigma_{12} \sqrt{x_1/l} \} \\
 \bar{p}_2^k &= \lim_{\bar{r} \rightarrow 0} \{ p_2^k \sqrt{\bar{r}/l} \} = \lim_{x_1 \rightarrow 0} \{ \sigma_{22} \sqrt{x_1/l} \}
 \end{aligned}
 \tag{5.28}$$

Thus, the stress intensity factors coincide with the tractions nodal values except

for a constant and may be computed directly with the boundary element code, i.e.

$$\begin{aligned} K_I &= \bar{p}_2^k (2\pi l)^{1/2} \\ K_{II} &= \bar{p}_1^k (2\pi l)^{1/2} \end{aligned} \quad (5.29)$$

Martinez and Dominguez [8] have shown how the use of the traction nodal values of the singular element at the crack tip (equation (5.29)) is substantially less sensitive to the discretization than any of the displacement correlation procedures.

Example 5.1

As an example, figure 5.7 shows the case of a centre cracked rectangular plate that has been studied by several authors [7], [8]. Because of the symmetry only one quarter of the plate is discretized. The total number of elements is nine, two of them being singular quarter-point elements. Plane stress is assumed and a Poisson's ratio $\nu = 0.2$. Figure 5.8 shows the error of the value computed for K_I using boundary elements versus the relative length of the singular quarter-point elements.

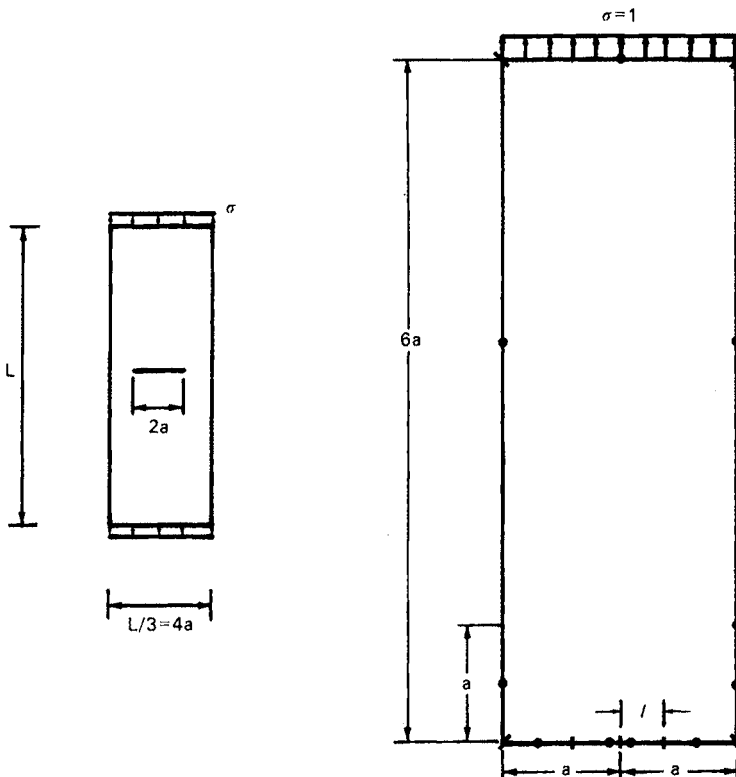


Figure 5.7 Centre cracked plate under traction. Discretization of one quarter of the plate.

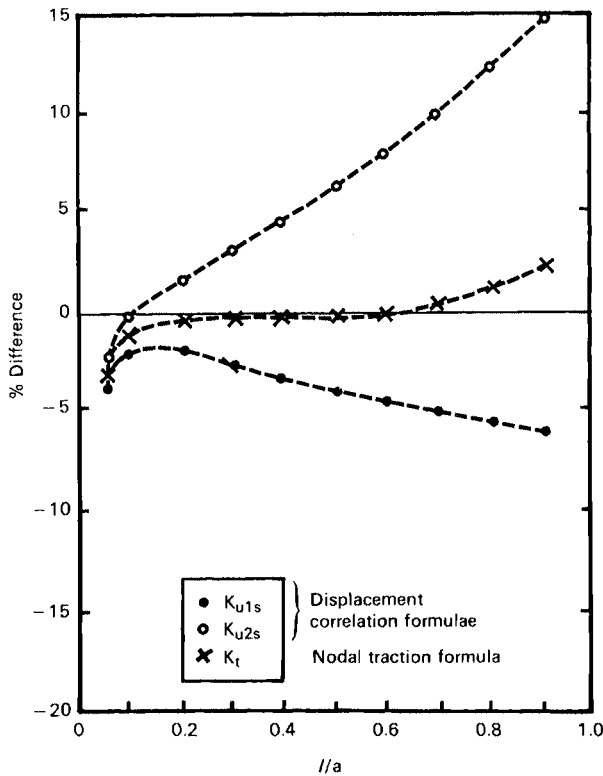


Figure 5.8 K_I stress intensity factor computed using quarter-point singular boundary elements

The value given by Bowie and Neal [8] is taken as reference as this value is accurate within one percent. The results obtained by the quarter-point boundary element procedure are given by K_t . Results computed using singular quarter-point elements and two different displacement correlation formulae (K_{u1s} and K_{u2s}) are given also for comparison. As can be seen in the figure, the nodal traction procedure with singular quarter-point elements (K_t) gives accurate results for a wide range of element sizes.

The implementation of a singular quarter-point element in the ELQUABE code of Chapter 4, requires only some minor changes in the integration routine.

5.5 Steady State Elastodynamics

Another interesting application of Boundary Elements which can be solved by modifying the codes presented in the previous chapters is the case of steady state elastodynamics. This is in a certain way similar to the harmonic wave propagation equation – or Helmholtz equation – discussed in section 2.14.

The equilibrium equations for an elastic region under dynamic loading can be written as,

$$\frac{\partial \sigma_{ij}}{\partial x_j} + b_i = \rho \ddot{u}_i \quad (5.30)$$

where \ddot{u}_i are the components of the acceleration. Substituting stresses in terms of displacements in the above formulae one obtains the dynamic expression of Navier's equation, i.e.

$$(\lambda + \mu)u_{j,ji} + \mu u_{i,jj} + b_i = \rho \ddot{u}_i \quad (5.31)$$

where λ and μ are the Lamé's coefficients. If all variables are considered as harmonic functions in time, with a frequency ω , equation (5.31) becomes

$$(\lambda + \mu)u_{j,ji} + \mu u_{i,jj} + b_i + \rho \omega^2 u_i = 0 \quad (5.32)$$

The boundary element formulation can be obtained as before using weighted residuals and when both the actual and weighting field are assumed to be harmonic, the integral equations become the same as for the static case, i.e.

$$c_{ki}^i u_k^i + \int_{\Gamma} p_{ki}^* u_k d\Gamma = \int_{\Gamma} u_{ki}^* p_k d\Gamma + \int_{\Omega} u_{ki}^* b_k d\Omega \quad (5.33)$$

where all the displacements, tractions and body forces are now frequency dependent. The fundamental solution corresponds to a point load with time variation $\exp(-i\omega t)$ and satisfies equation (5.32) without body forces, i.e.

$$(\lambda + \mu)u_{k,ki}^* + \mu u_{i,kk}^* + \rho \omega^2 u_i^* + \Delta_i(\omega) = 0 \quad (5.34)$$

For three dimensional problems this solution is given by

$$u_{ki}^* = \frac{1}{\alpha \pi \rho C_s^2} [\psi \delta_{ki} - \chi r_{,k} r_{,i}] \quad (5.35)$$

where $\alpha = 4$, C_s is the shear wave velocity, C_p the P -wave velocity, and the functions ψ and χ are

$$\begin{aligned} \psi = & \left(1 - \frac{C_s^2}{\omega^2 r^2} + \frac{C_s}{i\omega r} \right) \frac{\exp(-i\omega r/C_s)}{r} \\ & - \left(\frac{C_s^2}{C_p^2} \right) \left(-\frac{C_p^2}{\omega^2 r^2} + \frac{C_p}{i\omega r} \right) \frac{\exp(-i\omega r/C_p)}{r} \end{aligned} \quad (5.36)$$

$$\begin{aligned} \chi = & - \left(\frac{3C_s^2}{\omega^2 r^2} + \frac{3C_s}{i\omega r} + 1 \right) \frac{\exp(-i\omega r/C_s)}{r} \\ & - \left(\frac{C_s^2}{C_p^2} \right) \left(-\frac{3C_p^2}{\omega^2 r^2} + \frac{3C_p}{i\omega r} + 1 \right) \frac{\exp(-i\omega r/C_p)}{r} \end{aligned} \quad (5.37)$$

where

$$C_s = \sqrt{\frac{\mu}{\rho}} \quad \text{and} \quad C_p = \sqrt{\frac{(\lambda + 2\mu)}{\rho}}, \quad i = \sqrt{-1}$$

The tractions are given by the following relationships

$$p_{ki}^* = \frac{1}{\alpha\pi} \left\{ \left(\frac{d\psi}{dr} - \frac{1}{r} \chi \right) \left(\delta_{ki} \frac{\partial r}{\partial n} + r_{,k} n_i \right) - \frac{2}{r} \chi \left(n_k r_{,i} - 2r_{,k} r_{,i} \frac{\partial r}{\partial n} \right) - 2 \frac{d\chi}{dr} r_{,k} r_{,i} \frac{\partial r}{\partial n} + \left(\frac{C_p^2}{C_s^2} - 2 \right) \left(\frac{d\psi}{dr} - \frac{d\chi}{dr} - \frac{\alpha}{2r} \chi \right) r_{,i} n_k \right\} \quad (5.38)$$

The steady-state fundamental solution for two-dimensions is also given by equations (5.35) and (5.38) for the case $\alpha = 2$, and the following ψ and χ functions

$$\psi = K_0 \left(\frac{i\omega r}{C_s} \right) + \frac{C_s}{i\omega r} \left[K_1 \left(\frac{i\omega r}{C_s} \right) - \frac{C_s}{C_p} K_1 \left(\frac{i\omega r}{C_p} \right) \right] \quad (5.39)$$

and

$$\chi = K_2 \left(\frac{i\omega r}{C_s} \right) - \frac{C_s^2}{C_p^2} K_2 \left(\frac{i\omega r}{C_p} \right) \quad (5.40)$$

Functions K_0 , K_1 and K_2 are the modified Bessel functions of the second kind and order 0, 1 and 2 respectively.

Integral equation (5.33) can then be discretized into boundary elements in the same form as for elastostatics and the codes previously studied can be extended to elastodynamics simply by changing the fundamental solutions and the solutions to compute internal stresses and set all variables as complex. For instance codes ELCONBE and ELQUABE of Chapter 4 would only require changes in subroutines EXTINEC and LOCINEC or EXTINEQ and LOCINEQ in addition to the general changes in the definition of variables as complex.

It is worth pointing out that as the fundamental solution is frequency dependent the system $\mathbf{AX} = \mathbf{F}$ has to be formed and solved for each frequency. The numerical treatment of Bessel function in the two dimensional formulation also requires more care than the logarithm of the static problem, in particular for high and very low frequency values.

Some applications of the use of boundary element methods in steady state elastodynamics can be seen in the work of Domínguez and Alarcón [10] and Domínguez [11].

References

- [1] Brebbia, C. A. and Georgiou, P. Combination of Boundary and Finite Elements in Elastostatics, *Appl. Math. Modell.*, 3(2), June 1979.
- [2] Brebbia, C. A. and Walker, S. Simplified Boundary Elements for Radiation Problems, *Res. Note Appl. Math. Modell.*, 2(2), June 1978.

- [3] Irwin, G. R. Fracture, in *Encyclopaedia of Physics* (Ed. S. Flugge), Vol. VI, Springer-Verlag, 1958.
- [4] Snyder, M. D. and Cruse, T. A. Boundary Integral Equation Analysis of Anisotropic Cracked Plates, *Int. J. Fracture*, **11**, 315–328, 1975.
- [5] Stern, M., Becker, E. B. and Dunham, R. S. A Contour Integral Computation of Mixed-mode Stress Intensity Factors, *Int. J. Fracture*, **12**, 359–368, 1976.
- [6] Cruse, T. A. Two-dimensional BIE Fracture Mechanics Analysis, *Appl. Math. Modell.*, **2**, 287–293, 1978.
- [7] Blandford, G. E., Ingraffea, A. R. and Liggett, J. A. Two-dimensional Stress Intensity Factor Computations using the Boundary Element Method, *Int. J. Num. Meth. Eng.*, **17**, 387–404, 1981.
- [8] Martinez, J. and Dominguez, J. On the Use of Quarter-point Boundary Elements for Stress Intensity Factor Computations, *Int. J. Num. Meth. Eng.*, **20**, 1941–1950, 1985.
- [9] Bowie, O. L. and Neal, D. M. A Note on the Central Crack in a Uniformly Stressed Strip, *Eng. Fracture Mech.*, **2**, 181, 1970.
- [10] Dominguez, J. and Alarcón, E. Elastodynamics, in *Progress in Boundary Element Methods, Vol. 1* (C. A. Brebbia, Ed.), Pentech Press, London, 1981.
- [11] Dominguez, J. Dynamic Stiffness of Rectangular Foundations, *M.I.T. Research Report No. 1278-20*, Civil Eng. Dept., 1978.